Following the Dynamics of pH in Endosomes of Live Cells with SERS Nanosensors†

ARTICLE *in* THE JOURNAL OF PHYSICAL CHEMISTRY C · JANUARY 2010

Impact Factor: 4.77 · DOI: 10.1021/jp910034z

4 AUTHORS, INCLUDING:

Burghardt Wittig
Freie Universität Berlin
166 PUBLICATIONS **4,883** CITATIONS

SEE PROFILE

Following the Dynamics of pH in Endosomes of Live Cells with SERS Nanosensors†

Janina Kneipp,*,‡,§ Harald Kneipp,|| Burghardt Wittig,|| and Katrin Kneipp||,⊥

Federal Institute for Materials Research and Testing, Berlin, Germany, Chemistry Department, Humboldt University Berlin, Germany, Institute of Molecular Biology and Bioinformatics, Charité University Medicine Berlin, Germany, and Physics Department, Danish Technical University, Lyngby, Denmark

Received: October 20, 2009; Revised Manuscript Received: December 10, 2009

The surface enhanced Raman scattering (SERS) spectrum of a reporter molecule attached to gold or silver nanostructures, which is pH-sensitive, can deliver information on the local pH in the environment of the nanostructure. Here, we demonstrate the use of a mobile SERS nanosensor made from gold nanaoaggregates and 4-mercaptobenzoic acid (pMBA) attached as a reporter for monitoring changes in local pH of the cellular compartments of living NIH/3T3 cells. We show that SERS nanosensors enable the dynamics of local pH in individual live cells to be followed at subendosomal resolution in a timeline of cellular processes. This information is of basic interest for a better understanding of a broad range of physiological and metabolic processes as well as for a number of biotechnological applications.

Introduction

Raman spectroscopy has been revolutionized by letting the inelastic scattering process of photons with the vibrational quantum states take place in the close vicinity of metal nanostructures. Under these conditions, Raman scattering signals can be enhanced by more than 10 orders of magnitude. This effect of surface enhanced Raman scattering (SERS) is mainly related to increased local optical fields of the metal nanostructures which exist due to resonances with the collective electron oscillations in the metal. A second enhancement mechanism occurs due to so-called "chemical or electronic effects", where a molecule in contact with a metal (nanostructure) exhibits a "new (resonance) Raman process" with a larger cross section than that of a free molecule.[1−5] Since many years, SERS has been of particular interest for investigating biological molecules and structures.[6−9] The ability of very sensitive detection of Raman spectra from highly confined volumes makes SERS a very promising tool for studies in living cells.[7,9−14] Gold nanoparticles introduced into cells are nanosensors that can measure Raman signals from intrinsic cellular molecules in their environment. As another application, metal nanoparticles with a reporter molecule attached can act as labels that highlight cellular structures based on the surface enhanced Raman signature of the reporter. Compared to fluorescence labels, SERS labels can provide several advantages, particularly for live cell use.[8,14−16] If the SERS spectrum of a reporter molecule depends on the pH value in its environment, SERS nanosensors can act as a pH meter.[17−23]

SERS spectra measured from 4-mercapto benzoic acid (pMBA) show such pH dependence due to dissociation of the carboxyl group at higher pH values.[24] The line at 1423 cm^{-1} for pMBA on gold or 1380 cm^{-1} for pMBA on silver (see spectra in Figure 1) belongs to the COO^- stretching mode and can be used as an indicator for the dissociation of the carboxyl group at higher pH values. Signal ratios of the 1423 cm^{-1} or 1380 cm^{-1} line and an aromatic ring vibration at 1076 cm^{-1} can be used to infer information on pH values.[17−20]

Figure 1a explains the basic idea behind a mobile pH SERS sensor for applications in live cells using pMBA attached to gold nanoaggregates. The SERS spectrum of the reporter reflects the pH of the surrounding endosome. The concept of a SERS-based pH sensor can also be extended to two-photon excitation using surface enhanced hyper-Raman scattering (SEHRS) of pMBA on silver nanoaggregates.[12,20] Figure 1b displays one- and two-photon excited Raman scattering in a vibrational level diagram. The two-photon pH sensor based on the SEHRS spectrum of pMBA benefits from excitation in the near-infrared and exhibits a spectral signature that allows pH probing in a more acidic environment. For illustration, Figure 1b shows a SERS and a SEHRS spectrum measured by the nanosensor in different cellular compartments. The spectra indicate pH values between 6.5 and 6.9 (SERS) and 4.5 and 4.9 (SEHRS), respectively.

In a former paper,[20] we have demonstrated the capability of a mobile SERS sensor using pMBA on gold nanoaggregates to probe and to image pH values in the endosomal compartments of single cells using one- and two-photon excitation.

Here, we explore the dynamics of pH in the endosomal compartment of live cells using pMBA SERS nanosensors at one-photon excitation.

In particular, we look at whole-single cell pH images at different times after the uptake of the nanosensors and perform statistical analysis of the distribution of pH values in a larger population of cells. Information on the time development of pH in endosomes plays an important role in a number of pathologies, among them certain cancers, cystic fibrosis, and pathologies of the kidney.[25−28] It can be also of central interest for biotechnological processes, such as nonviral gene delivery.[29,30]

Experimental Section

The enhancing nanostructures for the pH sensor are gold nanoaggregates 80−120 nm in size formed by 3−5 gold spheres

* Corresponding author.
† Part of the "Martin Moskovits Festschrift".
‡ Federal Institute for Materials Research and Testing.
§ Humboldt University Berlin.
|| Charité University Medicine Berlin.
⊥ Danish Technical University.

10.1021/jp910034z
Published on Web 01/05/2010

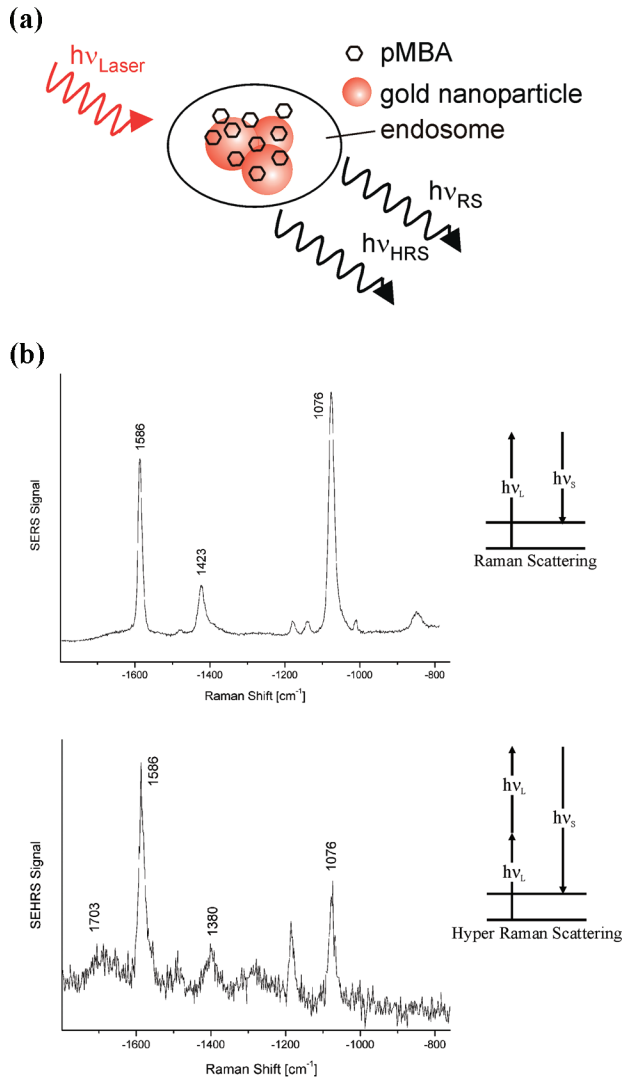

Figure 1. (a) Concept of SERS probing in cells. The mobile nanosensor is made from gold or silver nanoaggregates and pMBA attached as a pH sensitive reporter. (b) Raman and hyper-Raman scattering in a vibrational level diagram. The traces illustrate pH-sensitive SERS and SEHRS spectra measured in different endosomes using the gold and silver SERS sensor and one- and two-photon excitation, respectively.

of 30−50 nm diameter.[7,20] The gold particles were incubated with 10^{-5} M pMBA (Sigma) in aqueous solution. The pH value in the environment of the sensor is inferred from the signal ratio (height of the band) of two specific Raman lines at 1423 and 1076 cm^{-1} in comparison with a calibration curve generated from the nanosensor dispersed in aqueous solution of known pH.[17−20] The SERS signature of pMBA reversibly follows changes of the pH in the environment of the SERS sensor in the time scale of a few seconds.[17,20] For generating a pH image of a cell, calibrated signal ratios are displayed in a false color plot.[20]

Whole-single cell pH images were generated at different times after the uptake of the nanosensors. At the same time, the pH image represents a hyper spectral image of the cell, as can be demonstrated by the merge between pH and microscopy bright field images. Statistical analysis of the distribution of pH values is performed in groups of single cells with the same history of endocytotic uptake of the gold particles.

Cells of the cell line NIH/3T3 (mouse fibroblast cells) were grown in DMEM culture medium (Mediatech) with 10% fetal bovine serum (Invitrogen) and 1% penicillin/streptavidin, split and grown on flamed coverslips to confluence at 37 °C, 5% CO_2.

The nanosensors were delivered into the cells by fluid phase uptake. To this, the culture medium was replaced by a culture medium containing the nanosensor at a concentration of 10^{-12} M. Incubation with the nanosensors was performed over various time durations. Following incubation, the cells were washed thoroughly with PBS buffer. Raman spectra were acquired from live cells in this buffer. In agreement with previous studies, no evidence of cell death was found following incubation with the gold nanoaggregates. On microscope inspection, the cells continued to divide during and after incubation with the SERS sensor.[20]

For SERS probing and imaging of individual cells, we used a customized microspectroscopic Raman setup.[20] A single-stage spectrograph and a liquid nitrogen-cooled CCD detector were used for spectral dispersion and collection of the scattered light. For imaging, raster scans over single living cells were carried out with a computer-controlled x,y-stage in 2 μm steps at a laser spot size of $\sim 2 \times 10^{-8}$ cm^2 using 830 nm diode laser excitation of ≤ 2 mW.

At positions in the cells where nanosensors are present, surface-enhanced Raman spectra were measured in 1 s accumulation time per spectrum. Total collection times for whole-cell images are between 50 and 100 s. Such acquisition times are short enough to perform measurements on the time scales of endosomal uptake and transport processes occurring in a cell.

Results and Discussion

The bright field image in Figure 2a shows two NIH/3T3 cells after 1 h of incubation with the gold nanosensors. The presence of the gold nanoaggregates in the cell was verified from SERS signals measured during a raster scan over the cell. At the applied collection time and excitation intensities, no normal, unenhanced Raman signals can be observed, and the appearance of a surface enhanced Raman spectrum indicates the presence of a nanosensor. SERS spectra shown in the figure are examples for spectra measured in different endosomal compartments during the scan over the rectangle. As demonstrated before, pH values are inferred from the ratio of the lines at 1423 and 1076 cm^{-1}.[17,19,20] The false color plot of this calibrated ratio displays the pH values measured in the rectangle.

A comparison of the pH image and the bright field image shows that, after 60 min, endosomes containing the nanosensors have only partly spread over the volume of the cytoplasm. For those endosomes, the sensors reveal pH values between 6.9 and 6.2, indicating endosomes in an early stage.[31]

This is also supported by statistical analysis of pH values measured from a larger cell population of the same history. The diagram in Figure 2b shows that after an uptake duration of 60 min, about 80% of the sensors measure pH values between 6.6 and 6.9. Sixteen percent of the sensors indicate pH values between 6.5 and 5.9. The statistical analysis also identifies a few measurements (<5%) indicating pH up to 7.4. This can be explained by nanosensors at a very early stage of internalization, where the early endosome, in close proximity to the membrane, can have the same pH of the surrounding PBS buffer.

Figure 3 illustrates the situation after 4.5 h of incubation time. In accord with the assumption that nanosensor-containing endosomes are distributed all over the cytosol, a SERS signature of pMBA was measured in almost each of the spectra collected in the area of the cell. The pH image now represents also a

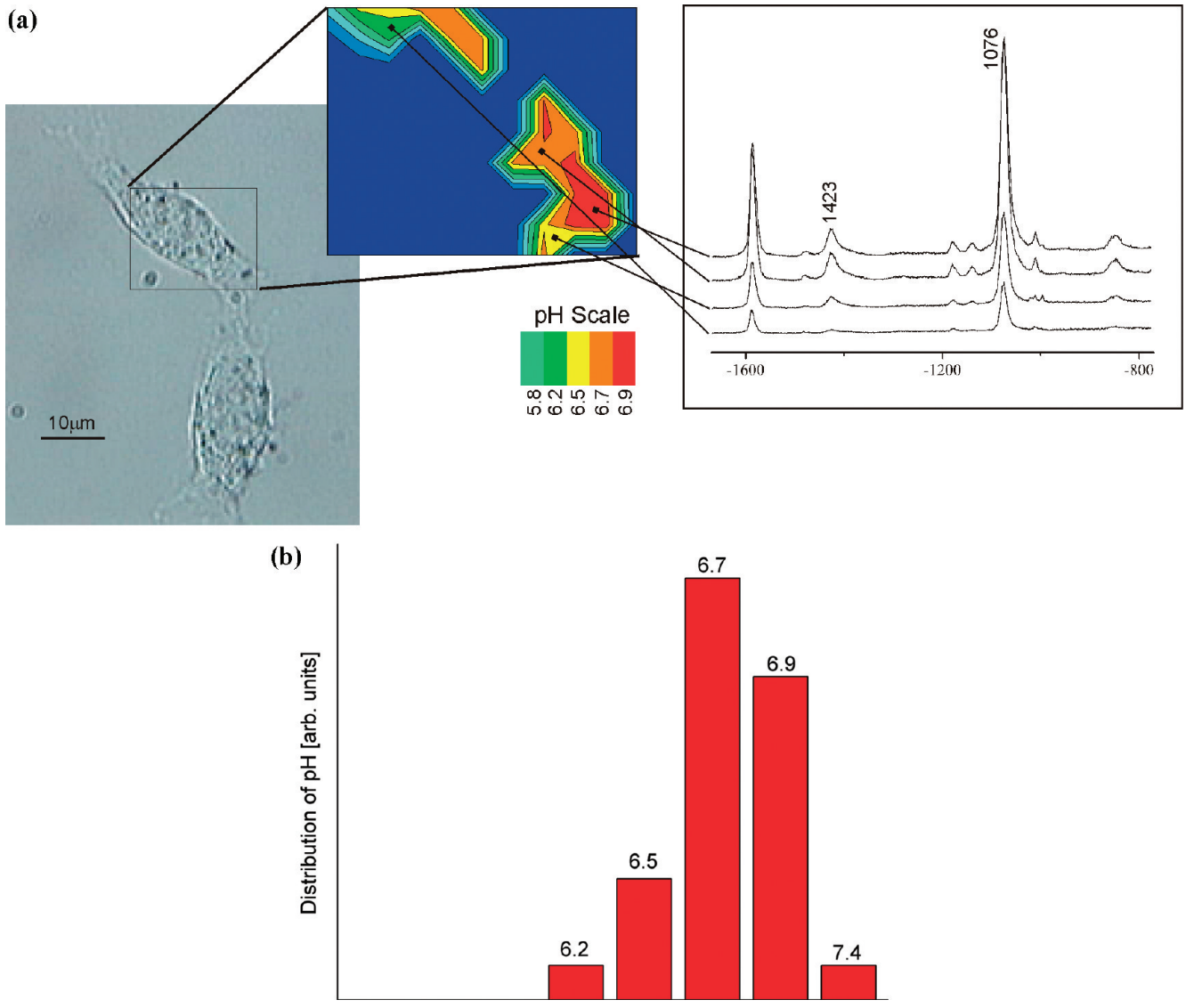

Figure 2. Probing and imaging pH in single live cells after 60 min of incubation time with SERS nanosensors. (a) The bright field image shows a 3T3 cell incubated with gold nanoparticles. The displayed SERS spectra are examples for spectra measured in different cellular compartments during a raster scan over the rectangle. The false color plot of the calibrated ratio of the Raman lines at 1423 and 1076 cm^{-1} displays a pH image of the cell. Scattering signals below a defined signal threshold, i.e., from places where no SERS signals exist, appear in dark blue. The values given in the color scale bar determine the upper end value of each respective color. (b) Distribution of pH based on SERS mapping over eight cells.

perfect hyperspectral image of the live cell as it can be seen from a comparison with the bright field image. Moreover, it shows variation of pH between 6.9 and 5 and maybe even below. This is in agreement with the presence of nanosensor-carrying endosomes of different ages in this experiment, where a portion of the nanosensors have been residing inside the cell already for more than 4 h. From ultrastructural studies of this and other cell lines, we know that, at this stage, many of the particles, which were taken up by the cells through the process of endocytosis, form accumulations in late endosomes and lysosomes.[11] This is reflected in cellular compartments that show pH between 6.2 and 5. At pH values around 5 and below, the COO^- stretching mode at 1423 cm^{-1} becomes too weak and can no longer be used as a pH indicator. Therefore, the pH range encoded in blue can also include much lower pH values. On the other hand, cells were exposed to the pH nanosensors continuously for 4.5 h until the Raman experiments were carried out. Therefore, in addition, a portion of the pH nanosensors must also be located in early endosomes. This explains that, in addition to more acidic cellular compartments, we have also parts of the cell showing pH values between 6.3 and 6.9.

The statistical pH distribution measured from single cells after 4.5 h of incubation (Figure 3b) confirms that the nanosensor occupies cellular compartments of all pH values between 6.9 and 5 and maybe even lower values, but still, there is a clear maximum for cellular compartments with pH values around 6.6 and 6.7 related to early endosomes. Again, in this experiment and also in Figure 4b, we find a few sensors indicating a surrounding pH of 7.4 corresponding to very early endosomes.

The data presented in Figure 4 were obtained from the same sample as that in Figure 3 but after an additional 90 min waiting period. A comparison between the pH images of the cell shown in Figure 3a and of the same cell 90 min later shown in the left lower quadrant of Figure 4a displays the dynamics in endosomal pH values. Cellular compartments appearing in Figure 3 in brown and red (pH 6.9−6.6) have now turned to yellow and green (pH 6.5−5.9), indicating the maturing process of endosomes. Interestingly, compartments in the same cell that show pH values between 5.5 and 5.8 (light green) show almost no changes between the images of Figures 3 and 4. The statistical analysis shown in Figure

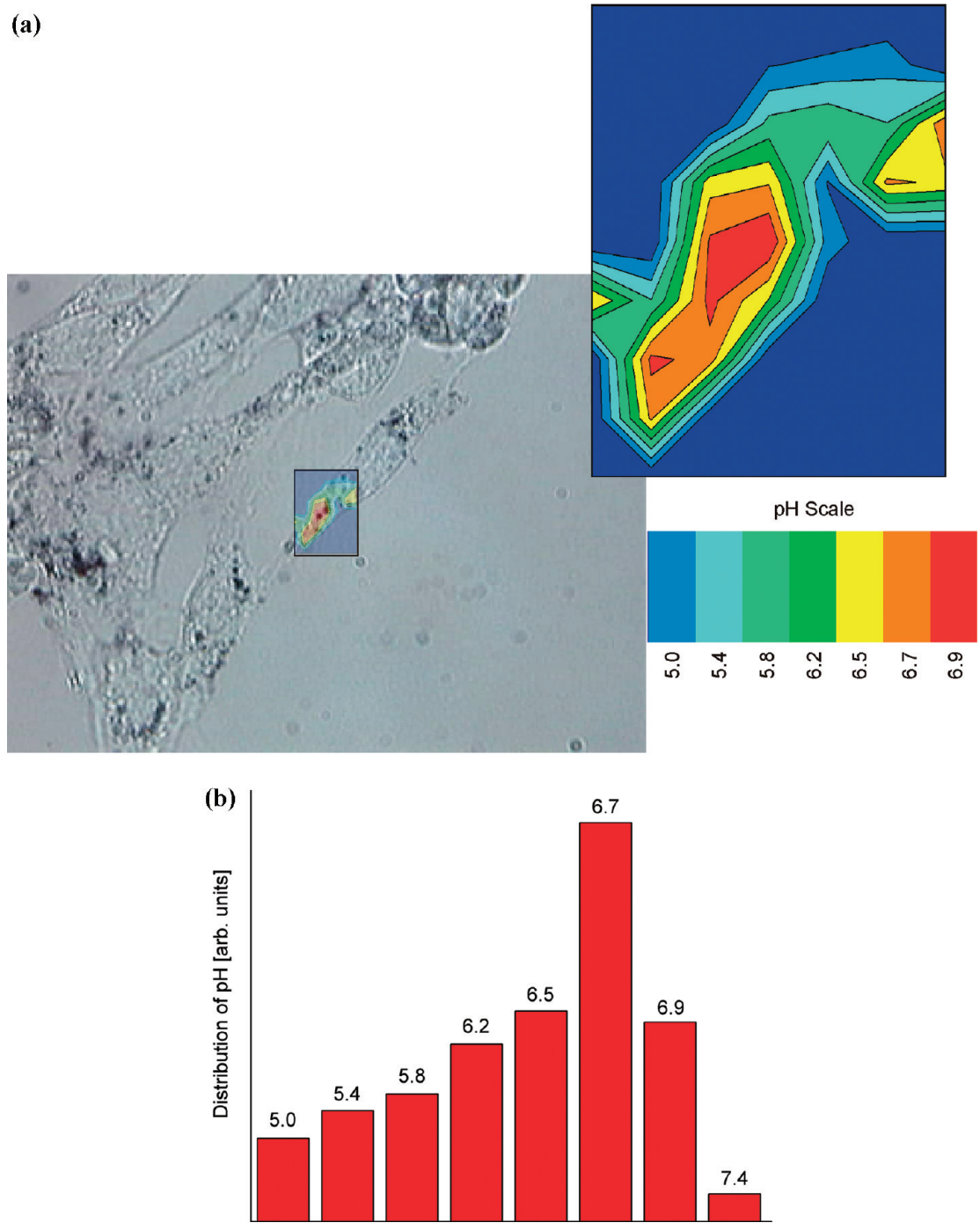

Figure 3. Probing and imaging pH in a single live 3T3 cell after 4.5 h of incubation time with SERS nanosensors. (a) pH image (rectangle 10 × 15 μm^2) merged with the bright-field image of the cell. The experimental conditions and procedures are the same as those in Figure 2. (b) Distribution of pH based on SERS mapping over five cells.

4b indicates a relatively uniform distribution over all pH values between 6.7 and 5. A few measurement points at pH values of 6.9 and 7.4 indicate the existence of early endosomes. This could be ascribed to gold nanosensors which had been taken up just before finalizing incubation shortly before the 90 min waiting time commenced.

Overall, a comparison between Figures 2−4 displays the dynamics of pH values in a live cell at subendosomal resolution. Our studies show that the gold nanoparticles used in our probes follow the pathway of all endocytosed materials. The statistical analysis of the distribution of pH values in groups of single NIH/3T3 cells with the same history of endocytotic uptake of the gold particles gives insight into the endosome maturation pathway. The changes in the distribution of pH values in a live cell can be explained by the maturation of endosomes after the endocytotic uptake of the gold nanosensor and the presence of nanosensor-carrying endosomes of different ages in our experiment. Our observation is in agreement with variation of pH measured in endosomes of different ages in this cell line.[31]

Conclusion

SERS nanosensors enable the dynamics of local pH in individual live cells to be followed at subendosomal resolution in a timeline of cellular processes. Monitoring pH in endosomal

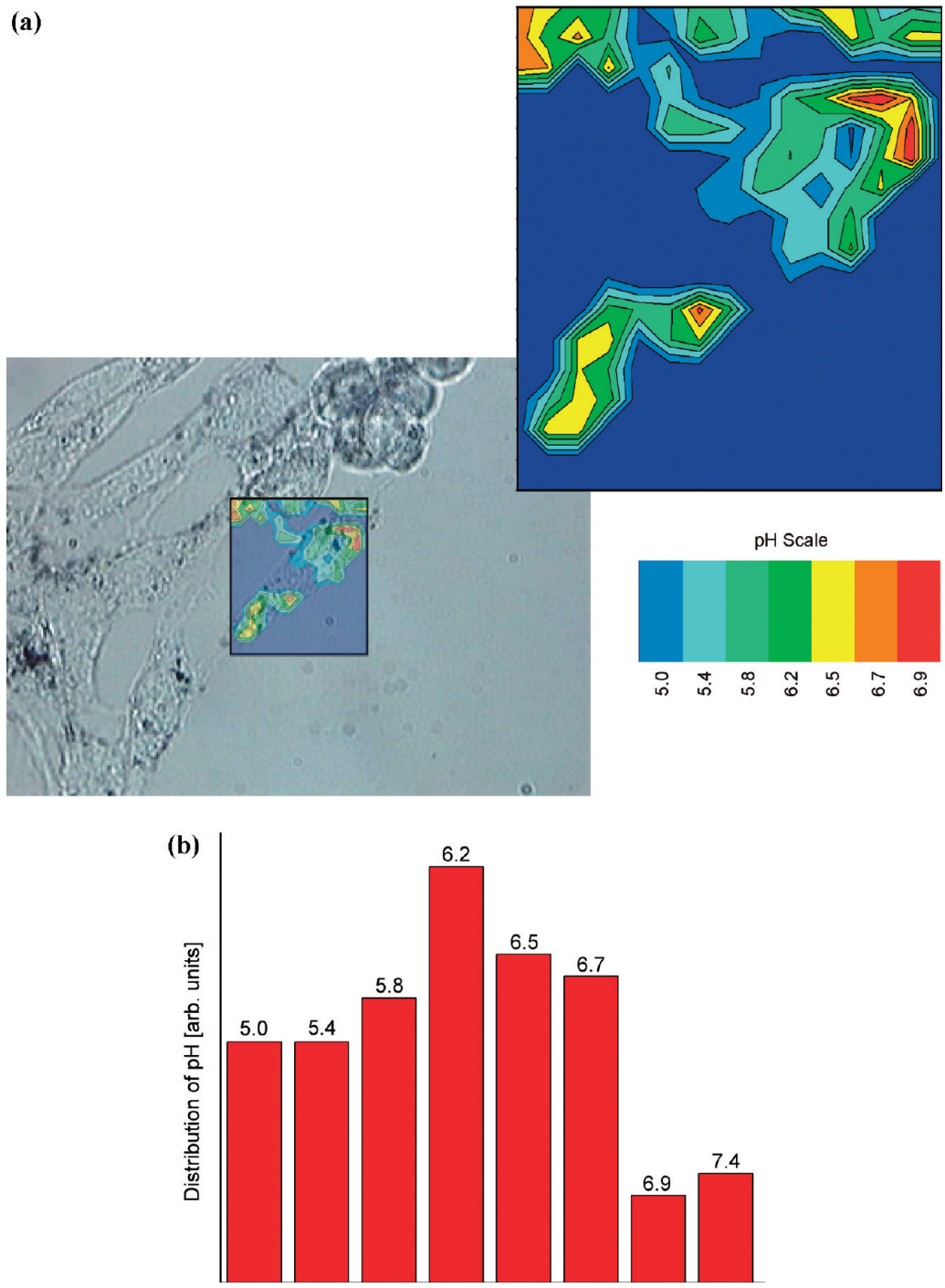

Figure 4. Probing and imaging pH of the same sample as shown in Figure 3 but 90 min later. (a) pH image (rectangle 30 × 26 μm^2) merged with the bright-field image. The experimental conditions are the same as those in Figures 2 and 3. The cell shown in Figure 3 is in the lower left quadrant of the scan. (b) Distribution of pH based on the scan shown in Figure 4a.

compartments over time is of basic interest for a better understanding of a broad range of physiological and metabolic processes[25−28] as well as for a number of biotechnological applications.[29,30]

As an advantage over pH sensors based on fluorescence, SERS pH sensors exploit the relative signals of pairs of Raman lines in the same spectrum. This allows quantitative measurements without any correction regarding optical cellular background signals. Moreover, the reporter pMBA provides strong signals under electronically nonresonant excitation. This avoids photodecomposition of the sensor and allows free selection of the excitation wavelengths.

The mobile nanosensors are distributed all over the cytosol. In this way, the pH image also represents a hyperspectral image of the live cell.

References and Notes

(1) Otto, A. Surface-enhanced Raman scattering: 'classical' and 'chemical' origins. In *Light scattering in solids IV. Electronic scattering, spin effects, SERS and morphic effects*; Cardona, M., Guntherodt, G., Eds.; Springer-Verlag: Berlin, 1984; Vol. 1984, pp 289−418.

(2) Moskovits, M. *Rev. Mod. Phys.* **1985**, *57*, 783–826.

(3) Dieringer, J. A.; McFarland, A. D.; Shah, N. C.; Stuart, D. A.; Whitney, A. V.; Yonzon, C. R.; Young, M. A.; Zhang, X. Y.; Van Duyne, R. P. *Faraday Discuss.* **2006**, *132*, 9–26.

(4) Kneipp, K., Moskovits, M., Kneipp, H., Eds. *Surface Enhanced Raman Scattering - Physics and Applications*; Springer: Heidelberg, Berlin, New York, 2006; Vol. 103.

(5) Kneipp, K. *Phys. Today* **2007**, *60*, 40–46.

(6) Kneipp, K.; Kneipp, H.; Itzkan, I.; Dasari, R. R.; Feld, M. S. *J. Phys.: Condens. Matter* **2002**, *14*, R597–R624.

(7) Kneipp, K.; Kneipp, H.; Kneipp, J. *Acc. Chem. Res.* **2006**, *39*, 443–450.

(8) Qian, X. M.; Nie, S. M. *Chem. Soc. Rev.* **2008**, *37*, 912–920.

(9) Kneipp, J.; Kneipp, H.; Kneipp, K. *Chem. Soc. Rev.* **2008**, *37*, 1052–1060.

(10) Kneipp, J. Nanosensors based on SERS for applications in living cells. In *Surface-Enhanced Raman Scattering: Physics and Applications*; Springer-Verlag: Berlin, 2006; Vol. 103, pp 335−349.

(11) Kneipp, J.; Kneipp, H.; McLaughlin, M.; Brown, D.; Kneipp, K. *Nano Lett.* **2006**, *6*, 2225–2231.

(12) Kneipp, J.; Kneipp, H.; Kneipp, K. *Proc. Natl. Acad. Sci. U.S.A.* **2006**, *103*, 17149–17153.

(13) Chourpa, I.; Lei, F. H.; Dubois, P.; Manfait, M.; Sockalingum, G. D. *Chem. Soc. Rev.* **2008**, *37*, 993–1000.

(14) Kneipp, J.; Kneipp, H.; Rajadurai, A.; Redmond, R. W.; Kneipp, K. *J. Raman Spectrosc.* **2009**, *40*, 1–5.

(15) Wabuyele, M. B.; Yan, F.; Griffin, G. D.; Vo-Dinh, T. *Rev. Sci. Instrum.* **2005**, 76.

(16) Kneipp, J.; Kneipp, H.; Rice, W. L.; Kneipp, K. *Anal. Chem.* **2005**, *77*, 2381–2385.

(17) Bishnoi, S. W.; Rozell, C. J.; Levin, C. S.; Gheith, M. K.; Johnson, B. R.; Johnson, D. H.; Halas, N. J. *Nano Lett.* **2006**, *6*, 1687–1692.

(18) Talley, C. E.; Jusinski, L.; Hollars, C. W.; Lane, S. M.; Huser, T. *Anal. Chem.* **2004**, *76*, 7064–7068.

(19) Schwartzberg, A. M.; Oshiro, T. Y.; Zhang, J. Z.; Huser, T.; Talley, C. E. *Anal. Chem.* **2006**, *78*, 4732–4736.

(20) Kneipp, J.; Kneipp, H.; Wittig, B.; Kneipp, K. *Nano Lett.* **2007**, *7*, 2819–2823.

(21) Jensen, R. A.; Sherin, J.; Emory, S. R. *Appl. Spectrosc.* **2007**, *61*, 832–838.

(22) Nowak-Lovato, K. L.; Rector, K. D. *Appl. Spectrosc.* **2009**, *63*, 387–395.

(23) Scaffidi, J. P.; Gregas, M. K.; Seewaldt, V.; Vo-Dinh, T. *Anal. Bioanal. Chem.* **2009**, *393*, 1135–1141.

(24) Michota, A.; Bukowska, J. *J. Raman Spectrosc.* **2003**, *34*, 21–25.

(25) Kokkonen, N.; Rivinoja, A.; Kauppila, A.; Suokas, M.; Kellokumpu, I.; Kellokumpu, S. *J. Biol. Chem.* **2004**, *279*, 39982–39988.

(26) Poschet, J. F.; Fazio, J. A.; Timmins, G. S.; Ornatowski, W.; Perkett, E.; Delgado, M.; Deretic, V. *EMBO Rep.* **2006**, *7*, 553–559.

(27) Hara-Chikuma, M.; Wang, Y. H.; Guggino, S. E.; Guggino, W. B.; Verkman, A. S. *Biochem. Biophys. Res. Commun.* **2005**, *329*, 941–946.

(28) Maranda, B.; Brown, D.; Bourgoin, S.; Casanova, J. E.; Vinay, P.; Ausiello, D. A.; Marshansky, V. *J. Biol. Chem.* **2001**, *276*, 18540–18550.

(29) Walker, G. F.; Fella, C.; Pelisek, J.; Fahrmeir, J.; Boeckle, S.; Ogris, M.; Wagner, E. *Mol. Ther.* **2005**, *11*, 418–425.

(30) Chowdhury, E. H.; Maruyama, A.; Kano, A.; Nagaoka, M.; Kotaka, M.; Hirose, S.; Kunou, M.; Akaike, T. *Gene* **2006**, *376*, 87–94.

(31) Murphy, R. F.; Powers, S.; Cantor, C. R. *J. Cell Biol.* **1984**, *98*, 1757–1762.

JP910034Z